Stability-Capacity-Adaptive Routing for High Mobility, Multi-Hop Cognitive Radio Networks

Xin-Lin Huang, *Student Member, IEEE,* Gang Wang, Fei Hu, *Member, IEEE,* and Sunil Kumar, *Senior Member, IEEE*

Abstract —In high-mobility cognitive radio networks (CRNs), the fast topology changes increase the complexity of routing scheme. In this paper, we propose a novel CRN routing scheme that considers the path stability and node capacity. First, a realistic mobility model is proposed to describe the movement of highly mobile airborne nodes (e.g., unmanned aerial vehicles (UAVs)), and estimate the link stability performance based on node movement patterns. Second, we propose a CRN topology management scheme based on a clustering model that considers radio link availability, and the cluster-heads (CHs) are selected based on the node degree level, average number of hops and channel switching from member nodes to the CH. Third, we propose two new common control channel (CCC) selection schemes based on the node contraction concept and the discrete particle swarm optimization (DPSO) algorithm. The inter-cluster control channels and gateways are selected from the CHs, considering the average delay of control information transmission between two CHs as well as the total throughput of control channels. Finally, a novel routing scheme is proposed that tightly integrates with channel assignment scheme based on the node capacity. Our simulation results show that our proposed CCC selection scheme has high throughput and small transmission time. Compared to other popular CRN routing approaches, our proposed routing scheme achieves lower average end-to-end delay and higher packet delivery ratio for *high-mobility* CRN applications (such as airborne surveillance).

Index Terms —Cognitive radio network (CRN), routing protocol, multi hop, high mobility, link stability, common control channel (CCC), clustering.

1 INTRODUCTION

Wireless communication is growing rapidly. However the wireless signals compete for the limited amount of spectrum in any given space. On the other hand, there exists much of the under-utilized licensed spectrum in many places, which has motivated the emergence of cognitive radio networks (CRNs) and dynamic spectrum access [1-3].

By opportunistically using the available spectrum in CRN, the devices can gain access to more wireless bandwidth without violating FCC regulations [3, 4]. Most of current CRN designs try to adapt the existing wireless network protocols while taking advantage of the dynamic spectrum access [5]. In a typical CRN, nodes are equipped with a spectrum-agile radio that has the capabilities of sensing the available spectrum bands, reconfiguring radio frequency, and switching to the selected new channels [6, 7].

_____

- *Xin-Lin Huang is with the Communication Research Center, Harbin Institute of Technology, Harbin 150001, P. R. China. E -mail: xlhitcrc@163.com.*
- *Gang Wang is with the Communication Research Center, Harbin Institute of Technology, Harbin 150001, P. R. China. E-mail: gwang51@hit.edu.cn.*
- *Fei Hu is with the department of Electrical and Computer Engineering, The University of Alabama, Tuscaloosa, AL 35487 USA. E-mail: fei@eng.ua.edu.*
- *Sunil Kumar is with the department of Electrical and Computer Engineering, San Diego State University, San Diego, CA 92182-1309 USA. E-mail: skumar@mail.sdsu.edu.*

In CRN routing protocol design, the *first* challenge is the integration of route discovery with the spectrum decision [2, 7, 8]. Due to the time-varying and intermittent spectrum availability, the spectrum channel information needs to be known (through spectrum sensing) when selecting the route. The *second* challenge is the lack of a stable common control channel (CCC). Since a CR node has to vacate the channel as soon as a primary user (PU) appears on that channel, the implementation of a fixed CCC may not be feasible. The *third* challenge is the spectrum-adaptive route failure recovery. In addition to node mobility, link failure in multi-hop CRN may happen when PU activities are detected around CRN users [7].

In this paper we design a *routing scheme for a multi-hop, high-mobility CRN* that overcomes the above three challenges. We consider an airborne surveillance network consisting of airborne nodes such as unmanned aerial vehicles (UAVs), as shown in Fig. 1. Different types of airborne nodes fly at different heights to carry out various surveillance and reconnaissance missions. We assume each node carries two CR transceivers to transmit data and control information. Our goal is to design a robust CRN routing protocol for this scenario to share information among airborne nodes, considering path stability (a low-mobility link has higher path stability) and node capacity (CR users with high processing capability will be selected as relay nodes). Our CRN routing design considers the node characteristics, cluster-head (CH) selection metric, control channel forming metric, and routing metric. The main feature of our proposed scheme is its capability to adapt to high-

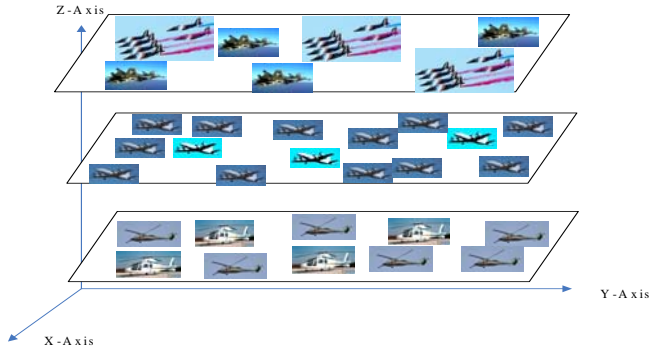mobility, multi-hop, and heterogeneous CRN environments.

Fig.1: High-mobility CRN application scenario.

In a CRN, the PUs have absolute high priority to use the licensed channels. The secondary users (i.e., airborne nodes) detect and use the spectrum unused by PUs, and should immediately vacate the channel if a PU re-occupies it.

We organize the nodes into clusters in order to reduce routing overhead. Despite the nodes' high mobility, the cluster structure should be as stable as possible when the cluster membership changes, especially when a CH changes. These changes adversely affect the performance of radio resource allocation and scheduling protocols [12]. In conventional ad-hoc networks, two popular clustering algorithms have been proposed, i.e., *Max Node Degree* clustering algorithm [13], and *Lowest ID* clustering algorithm [14]. However, *these algorithms do not consider the heterogeneity of available channels, i.e., each channel may have a different link availability probability.* Therefore, we design a new clustering scheme for CRNs that can adapt to the link availability characteristics.

In a CRN, it is imperative to select a CCC for exchanging the control information among nodes. A CCC selection scheme based on swarm intelligence was proposed in [15], which tries to form a local control channel in the network. Another local control channel selection scheme was proposed in [16] and [17], which exchanges control information in a cooperated group or cluster. A novel control channel selection scheme was proposed in [18], which tries to form a control channel along the routes. However, these CCC selection schemes do not consider the transmission delay and throughput. In this paper, we propose a novel CCC selection scheme based on a new concept called 'node contraction', which can quickly select a high-quality CCC among CHs.

Based on the cluster structure and CCC selection scheme, a routing protocol can be established efficiently. Recently, several routing schemes have been proposed for multi-hop CRNs. For example, a spectrum-tree-based on-demand routing protocol (STOD-RP) was proposed in [7]. In STOD-RP, all nodes are assumed to be stationary or move very slowly, and the statistics of PU activities and available spectrum band information are assumed to be always available. A spectrum aware on demand routing

protocol (SORP) is proposed in [8]. SORP considers the inter-flow interference and channel switching delay, and is a cumulative-delay-based routing protocol. However, it cannot adapt to mobile environment very well. In [19-22], Quality of Service (QoS) based routing is widely studied. In [23, 24], the interference is considered in routing design. Again, they do not tightly integrate CRN routing with node mobility for a highly mobile scenario.

In fact, there is very little research on the routing algorithms for *high-mobility* CRNs. Especially, little work has been done to design a CRN routing scheme based on the measurement of path stability (which, in turn, depends on node mobility) and node capacity. Although the path and cluster stability have been studied widely (such as [9, 12, 25-28]) for MANET (mobile ad hoc networks), they do not consider the dynamic spectrum assignment and spectrum heterogeneity in CRN environment.

The rest of the paper is organized as follows. In Section 2, we present a cluster formation scheme which uses node characteristics to achieve flexible CRN topology management. In Section 3, we propose efficient common control channel (CCC) selection schemes, which are important for CRN routing management. In Section 4, we discuss our CRN routing establishment and failure recovery method. We also propose new CRN routing metrics to measure the path quality. In Section 5, the extensive experimental results are presented. Finally, we conclude this paper in Section 6.

2 NODE CHARACTERISTICS AND CLUSTER FORMATION IN HIGH-MOBILITY CRN

2.1 CRN Node Mobility Model

To design a routing protocol, we need a mobility model to realistically represent the node mobility patterns. The popularly used random mobility models (such as random walk mobility model, random waypoint mobility model, random direction mobility model, and Gauss-Markov mobility model [9-11]) do not suit our scenario since the airborne nodes do not use random paths.

We use the bird flocking mobility model to describe the movement trajectories of airborne nodes. In this mobility model, the nodes do not move randomly and there is an intrinsic rule behind their formation. For example, the birds do not collide and the shape of their formation follows leader-follower pattern. The airborne nodes fly in a formation with certain range and heights to accomplish the given surveillance tasks. We discuss the basic bird flocking model below [29].

Suppose S represents the population of bird flock and D represents the dimension of flying space. The position of the bird i at time kT (T is the unit time) is $x_i^{kT} = [x_{i1}^{kT}, x_{i2}^{kT}, ..., x_{iD}^{kT}]$, with velocity $v_i^{kT} = [v_{i1}^{kT}, v_{i2}^{kT}, ..., v_{iD}^{kT}]$. Let $p_i^{kT} = [p_{i1}^{kT}, p_{i2}^{kT}, ..., p_{iD}^{kT}]$ represent the *personal best position (PBP)* of bird i, and $p_b^{kT} = [p_{b1}^{kT}, p_{b2}^{kT}, ..., p_{bD}^{kT}]$ represent the *global best position (GBP)* of the flock,

where b is the index of the bird with the GBP. The best position may be the shortest distance to the destination (a formation convergence position). Therefore, the mobility model of bird i is determined by its speed and location [29]:

$$v_{id}^{(k+1)T} = \omega v_{id}^{kT} + c_{1d} r_1 (p_{id}^{kT} - x_{id}^{kT}) + c_{2d} r_2 (p_{bd}^{kT} - x_{id}^{kT}) \quad (2.1)$$

$$x_{id}^{(k+1)T} = x_{id}^{kT} + v_{id}^{(k+1)T} T \quad (2.2)$$

where v_{id}^{kT} is the current speed and x_{id}^{kT} is the current location of bird i at time kT, d represents the dimension of the position, and ω is an inertial weight coefficient (usually we set $\omega = 1$). In the *update* process, the bird's speed is limited to a range $v_{id}^{kT} \in [-V_{max}, V_{max}]$ in each dimension, where $-V_{max}$ (negative speed) represents the speed in the opposite direction of the global axis. c_{1d} and c_{2d} are the learning factors, and $c_{1d} = c_{2d} = V_{max} / L_d$, where L_d is the side length of the d th dimension. r_1 and r_2 obey uniform distribution over [0,1].

In equation (2.1), the current speed of bird i consists of three parts: the first part is previous speed, which can be interpreted as the result of inertial motion; the second part is a cognitive part, which means that the bird changes its speed according to its own flying experience; and the third part represents the social consistence and interactions [29].

We use equations (2.1) and (2.2) to model the mobility characteristics of airborne nodes. As an example, Fig. 2 shows the movement traces for 10 nodes, flying to search a target. Here, the black empty circles represent the initial node positions; red empty circles represent the positions after 500 seconds; and the star represents the target (i.e., convergence position). T is set to 100 seconds and $V_{max} = 10 \, \mathrm{m/s}$ (i.e., 36km/h). Note that the airborne nodes on a surveillance and reconnaissance mission usually fly at stable speed to easily detect the target. *From Fig. 2, we see that the bird flocking mobility model describes a mission-specific movement trajectory very well* as the nodes move closer to the target with time.
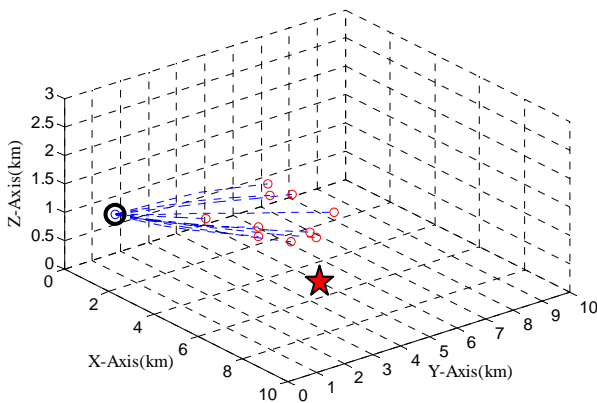

Fig. 2: Example movement trace, 500 seconds after the start of simulation.

2.2 CRN Spectrum Heterogeneity

We assume that the CRN consists of N secondary users (i.e., CRN nodes) and M orthogonal spectrum channels. The spectrum available to CRN users can be described in terms of *channel availability*, *channel reward* and *interference constraint* as defined below [30]. The channel availability and rewards for each CRN user is calculated based on the location and channel usage of nearby PUs.

- *Channel availability*: $L = \{l_{n,m} \,|\, l_{n,m} \in \{0,1\}\}_{N \times M}$ is a N by M binary matrix, where $l_{n,m}$ represents the availability of channel m to user n. $l_{n,m} = 1$ if and only if channel m is available to secondary user n.

- *Channel rewards*: $B = \{b_{n,m}\}_{N \times M}$ is a N by M matrix, where $b_{n,m}$ represents the maximum bandwidth/throughput that can be acquired (assuming no interference from neighbors) by user n that is using channel m. The channel reward can be defined as the coverage of a secondary user (n) using a channel (m) [30]:

$$b_{n,m} = d_s(n,m)^2, \; d_{min} \leq d_s(n,m) \leq d_{max}$$

Each secondary user n can adjust its interference range $d_s(n,m)$ by tuning its transmit power on channel m to avoid interfering with PUs.

We assume that each secondary user can use only one channel at a time [31]. A node cannot use the maximum transmit power to search its neighbors, except when it cannot receive any information from its neighbors. Only the CHs are allowed to communicate with each other at the maximum transmit power. We assume that a secondary user broadcasts its information in a coverage radius of R_0 during cluster formation, and tunes its transmit power to connect with its neighbors according to their distance level.

- *Interference constraint*: $C = \{c_{n,k,m} \,|\, c_{n,k,m} \in \{0,1\}\}_{N \times N \times M}$ is a N by N by M matrix, and represents the interference constraint among secondary users. If $c_{n,k,m} = 1$, users n and k would interfere with each other if they use channel m for data transmission simultaneously. The constraint is determined by channel availability, transmit power, and distance between users n and k.

2.3 Link Availability

In a CRN, the link availability between node A and B on channel m is defined as [32]:

$$d_s(A,m) > Dis(A,B) \text{ and } d_s(B,m) > Dis(A,B),$$
$$\text{when } l_{A,m} = l_{B,m} = 1 \quad (2.3)$$

If the link between nodes A and B is available on channel m at time $kT + t_0$ ($0 \leq t_0 \leq T$), i.e., $Link_{A,B,m}(kT + t_0) = 1$, the probability of availability in this link at time $kT + t_0 + T_p$ (T_p is data transmitting time of a flow) can be expressed as [33-36]:

$$\Pr\{Link_{A,B,m}(kT+t_0+T_p)=1, \ under \ the \ condition - V_{\max} \le v_{id}^{kT+t_0+T_p} \le V_{\max} \ for \ node \ A \ and \ node \ B, d=1,2,..,D\}$$

$$\le \frac{\Pr\{Link_{A,B,m}(kT+t_0+T_p)=1\}}{\Pr\{-V_{\max} \le v_{id}^{kT+t_0+T_p} \le V_{\max}, d=1,2,..,D\}\Big|_{node\ A} \cdot \Pr\{-V_{\max} \le v_{id}^{kT+t_0+T_p} \le V_{\max}, d=1,2,..,D\}\Big|_{node\ B}} \tag{2.4}$$

where

$$\Pr\{Link_{A,B,m}(kT+t_0+T_p)=1\}$$

$$= \Pr\{\sum_{d=1}^{D}(x_{id}^{kT+t_0}\Big|_{node\ A} + T_p v_{id}^{(k+1)T}\Big|_{node\ A} - x_{id}^{kT+t_0}\Big|_{node\ B} - T_p v_{id}^{(k+1)T}\Big|_{node\ B})^2 < \min\{d_s^2(A,m), d_s^2(B,m)\}\}$$

$$\le \Pr\{\Big|[\sum_{d=1}^{D}(x_{id}^{kT+t_0}\Big|_{node\ A} + T_p v_{id}^{(k+1)T}\Big|_{node\ A} - x_{id}^{kT+t_0}\Big|_{node\ B} - T_p v_{id}^{(k+1)T}\Big|_{node\ B})]\Big| < \sqrt{D \times \min\{d_s^2(A,m), d_s^2(B,m)\}}\} \tag{2.5}$$

$$\approx \Phi\{\frac{\sqrt{D \times \min\{d_s^2(A,m), d_s^2(B,m)\}} - \mu_1}{\sigma_1}\} - \Phi\{\frac{-\sqrt{D \times \min\{d_s^2(A,m), d_s^2(B,m)\}} - \mu_1}{\sigma_1}\}$$

$$\mu_1 = \sum_{d=1}^{D}(x_{id}^{kT+t_0}\Big|_{node\ A} + T_p[v_{id}^{kT} + \frac{c_1}{2}(p_{id}^{kT} - x_{id}^{kT}) + \frac{c_2}{2}(p_{bd}^{kT} - x_{id}^{kT})]\Big|_{node\ A} - x_{id}^{kT+t_0}\Big|_{node\ B} - T_p[v_{id}^{kT} + \frac{c_1}{2}(p_{id}^{kT} - x_{id}^{kT}) + \frac{c_2}{2}(p_{bd}^{kT} - x_{id}^{kT})]\Big|_{node\ B})$$

$$\delta_1 = \sqrt{\sum_{d=1}^{D}(T_p^2[c_1^2(p_{id}^{kT} - x_{id}^{kT})^2 + c_2^2(p_{bd}^{kT} - x_{id}^{kT})^2]\Big|_{node\ A} + T_p^2[c_1^2(p_{id}^{kT} - x_{id}^{kT})^2 + c_2^2(p_{bd}^{kT} - x_{id}^{kT})^2]\Big|_{node\ B})/12}$$

$$\Phi(x) = \frac{1}{\sqrt{2\pi}}\int_{-\infty}^{x}\exp(-\frac{t^2}{2})dt$$

and

$$\Pr\{-V_{\max} \le v_{id}^{kT+t_0+T_p} \le V_{\max}, d=1,2,..,D\}\Big|_{node\ A} \cdot \Pr\{-V_{\max} \le v_{id}^{kT+t_0+T_p} \le V_{\max}, d=1,2,..,D\}\Big|_{node\ B} \tag{2.6}$$

$$= \prod_{d=1}^{D}\Pr\{-V_{\max} \le v_{id}^{kT+t_0+T_p} \le V_{\max}\}\Big|_{node\ A} \cdot \prod_{d=1}^{D}\Pr\{-V_{\max} \le v_{id}^{kT+t_0+T_p} \le V_{\max}\}\Big|_{node\ B}$$

$$\Pr\{-V_{\max} \le v_{id}^{kT+t_0+T_p} \le V_{\max}\} = \begin{cases} 1, & if \ p_{id}^{kT} = x_{id}^{kT} \ and \ p_{bd}^{kT} = x_{id}^{kT} \\ \Phi(\frac{V_{\max}-\mu_2}{\delta_2}) - \Phi(\frac{-V_{\max}-\mu_2}{\delta_2}), \ others \end{cases}$$

$$\mu_2 = v_{id}^{kT+t_0} + \frac{c_1}{2}(p_{id}^{kT} - x_{id}^{kT}) + \frac{c_2}{2}(p_{bd}^{kT} - x_{id}^{kT})\Big|_{node\ A\ or\ B}$$

$$\delta_2 = \sqrt{[c_1^2(p_{id}^{kT} - x_{id}^{kT})^2 + c_2^2(p_{bd}^{kT} - x_{id}^{kT})^2]\Big|_{node\ A\ or\ B}/12}$$

In equation (2.5) and (2.6), we have used Lyapunov's central limit theorem [37] and inequality $x_1^2 + x_2^2 + \ldots + x_D^2 \ge (x_1 + x_2 + \ldots + x_D)^2/D$. μ_1 and μ_2 represent mean values, while δ_1 and δ_2 represent variances. For simplicity, we use the upper bound to represent the link availability probability.

2.4 Cluster Formation

The clustering can reduce the network scale and thus the routing protocol overhead [38]. Clustering in MANETs typically need to consider energy metric, average distance, and node degree. *However, clustering in CRN should consider the spectrum heterogeneity.* Since the airborne nodes in our scenario move in a formation using predictable orbits at stable speeds, the topology is relatively stable despite high node speeds. Furthermore the airborne nodes can communicate with each other over

longer distances (i.e., within 3 km) using line of sight path which makes the cluster formation possible. We assume that each cluster's coverage is 2 hops. However, this could be easily adapted to k-hop case in our algorithm.

To ensure a cluster's longevity, the probability of link availability must be greater than certain value, denoted as P_0 , during a time period $[kT,(k+1)T]$. This would ensure that the cluster topology remains stable for a long enough period of time (T). Our clustering scheme not only takes into account spectrum heterogeneity, node degree and intra-cluster delay, but also the stability of topology. *We introduce a new metric called "node importance degree $\alpha_{i,m}$"*, which is defined as,

$$\alpha_{i,m} = \frac{n_{i,m}}{1 + \frac{1}{n_{i,m}}\sum_{j=1}^{n_{i,m}}hop_j + \frac{1}{n_{i,m}}\sum_{j=1}^{n_{i,m}}Switch_j} \tag{2.7}$$

where $n_{i,m}$ represents the number of 2-hop neighbors of node i on channel m, $\frac{1}{n_{i,m}}\sum_{j=1}^{n_{i,m}} hop_j$ is the average number of hops from all 1-hop and 2-hop neighbors to node i, and $\frac{1}{n_{i,m}}\sum_{j=1}^{n_{i,m}} Switch_j$ is the average channel switching steps.

Example: We explain our clustering scheme using Fig. 3. It has six CRN users with different available channels. A node's neighbors are determined by its transmission range as well as the channel being used. *The node with the largest node importance degree is selected as CH.* Initially, each node broadcasts its available channel set, location, speed, the best position and mobility characteristics (i.e., the PBP and GBP discussed in Section 2.1), in each available channel. When a node collects all its 2-hop neighbors' information, the topology is formed as shown in Fig. 3. Then, each node calculates its largest node importance degree by using equation (2.7) as shown in Table 1 for each available channel. In Table 1, Node 1 has the largest node importance degree on channel 1. Thus we choose node 1 as CH and channel 1 is used as the intra-cluster control channel. In the cluster formation process, each node will select the node with the largest "node importance degree" within its 2-hop neighborhood as its CH. Since node 4 cannot use channel 1, node 3 acts as a switching node for it, and works on channel 1 and 2.

Since the cluster formation considers only the local information, the following two issues should be considered: (1) the selected CH may not be able to connect with other CHs, and (2) the assigned channel (e.g., channel 1 for node 1 in Fig. 3) may be occupied by inter-cluster communication or PUs later on. To solve these two issues, we propose an enhanced node-importance-based CRN clustering scheme as follows:
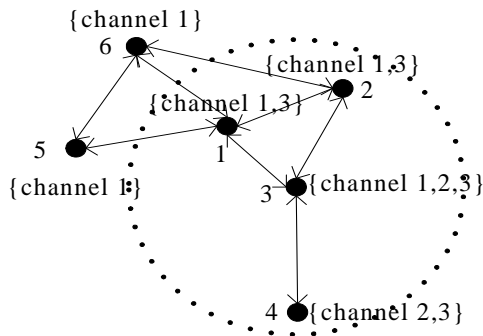

Fig. 3: Topology of a cluster.

After cluster formation, the CH broadcasts its available channel and member list to other CHs on each available channel with maximum transmit power. When the CH does not hear response from other CHs, it knows that other CHs are out of its coverage area. If a CH's intra-cluster control channel is occupied by other users later on, another channel or a new CH must be selected. In these two situations, we select a member node with *the next*

largest node importance degree as CH. This new CH must be able to operate on the inter-cluster control channel and connect with other CHs.

Table 1: Node Importance Degree $\alpha_{i,m}$ for Each Node in Available Channels

Node Number	Available Channel	Node Importance Degree $\alpha_{i,m}$	Node Degree $n_{i,m}$
1	1	2.08	5
	3	1.29	4
2	1	1.92	5
	3	1.33	5
3	1	1.60	4
	2	0.50	1
	3	1.56	5
4	2	0.90	3
	3	1.13	3
5	1	1.60	4
6	1	1.78	4

Since the coverage of a CH is 2-hop neighbors, the CH and its 1-hop neighbors may switch to different channels. In this situation, a *deaf* problem will occur. A node must send Join-message and Leave-message over the control channel before it switches to another channel.

3. CONTROL CHANNEL SELECTION

A good CCC is very important to coordinate the channel allocation among CRN nodes. Due to the time varying nature of channel availability in CRN, the ability to quickly select a new CCC is also needed when the current control channel is jammed or re-occupied by PUs. However, in a large-scale CRN, a *global* CCC is rarely available for all nodes [16]. Therefore, a natural choice is to select local CCCs in different clusters. We also need to form a CCC among different CHs. Since the CCC selection is a spectrum resource assignment problem, it is an *NP-hard* problem [30].

In order to solve the CCC selection issue, *we introduce two parameters below: (1) average control information transmission delay* (we simply call it *Delay* in future discussions), and *(2) the throughput of control channel* (denoted as U_{sum}). Suppose the CRN consists of I CHs, which are denoted as $H_0, H_1, \ldots, H_{I-1}$. Let t_{hop} and t_{sw} represent the 1-hop transmission delay and channel switch delay [39, 40], respectively. The 1-hop transmission delay contains queuing delay, packets transmission time, protocol overhead [40]. Let the path between the CH H_i and H_j consist of $d_{i,j}$ hops and $s_{i,j}$ channel switching steps. The control information transmission delay between CHs H_i and H_j is $d_{i,j} \times t_{hop} + s_{i,j} \times t_{sw}$. The minimum control information transmission delay is

$$Delay = \frac{1}{I \times (I-1)/2} \sum_{i=0}^{I-1} \sum_{j=i+1}^{I-1} \min(d_{i,j} \times t_{hop} + s_{i,j} \times t_{sw}) \quad (3.1)$$

This article has been accepted for publication in a future issue of this journal, but has not been fully edited. Content may change prior to final publication.

6   TO IEEE TRANSACTIONS ON VEHICLE TECHNOLOGY

The *throughput* of control channel can be determined as [30]:

$$U_{sum} = \sum_{n=0}^{I-1} \frac{\sum_{m=0}^{M-1} a_{n,m} \cdot b_{n,m}}{\sum_{m=0}^{M-1} a_{n,m}} \tag{3.2}$$

where $a_{n,m} = 1$ means that CH n uses channel m as the control channel, and $b_{n,m}$ is the corresponding channel reward as discussed in Section 2.2. M is the number of available channels.

Using these two parameters, we propose two control channel selection schemes: *the node contraction scheme (Section 3.1) and the discrete particle swarm optimization (DPSO) scheme (Section 3.2)*. The optimization function is given as,

$$F = \chi(1 - \frac{Delay}{(I-1)t_{hop} + (M-1)t_{sw}}) + \\ (1-\chi) \frac{U_{sum}}{I \times \max\{b_{n,m}, n \in \{0,1,\ldots,I-1\}, m \in \{0,1,\ldots,M-1\}\}} \tag{3.3}$$

where χ is weighted coefficient, and $\chi \in [0,1]$.

3.1 Node Contraction Scheme

Since nodes in our scenario (Fig. 1) move fast and the emergence of PUs is unpredictable (considering many types of wireless networks deployed today), the control channel established on spectrum opportunistic (SOP) basis may have to be switched from time to time. In a CRN application, the control channels must be established and restored in a short time. In this section, we propose a *node contraction* scheme to establish the control channel quickly. The *node contraction* method was first proposed in [41] to illustrate the node importance in power system control.

The flow chart of our scheme is shown in Fig. 4. At each stage, the algorithm labels each CH n with a spectrum band m as $label(n,m) = b_{n,m}$, where $b_{n,m}$ is *channel reward* as discussed in Section 2.2. The algorithm selects the CH with the highest valued *label* with spectrum band m, and contracts all neighboring CHs to it. Thus a new CH is formed. The algorithm removes the new CH from CRN and enters the next stage until running through all the CHs.

Example: This scheme is illustrated in Fig. 5. Assuming the CH H_4 with spectrum band 1 has the largest valued *label*, the CHs $H_0, H_1, H_2, H_3, H_4, H_6, H_7$ contract to this new CH, named as $H_4 *$. We remove $H_4 *$ from the CRN. Next, the CH H_{10} has the largest valued *label*, and the CHs H_8, H_9, H_{10}, H_{11} contract to it. All CHs are removed from the CRN one-by-one in this way.

Note that the node contraction is only the first step in CCC determination. In the next step, we need to select *gateways* from the new CHs. The gateways guarantee that

two neighboring clusters share a CCC. In Fig. 5, the CHs H_4, H_6, H_7 could be selected as gateways. The best gateway set is selected based on the optimization function in equation (3.3).
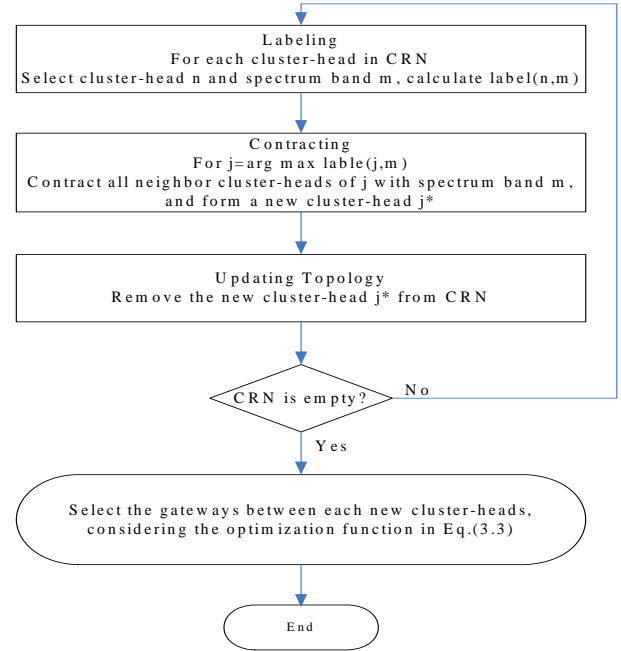

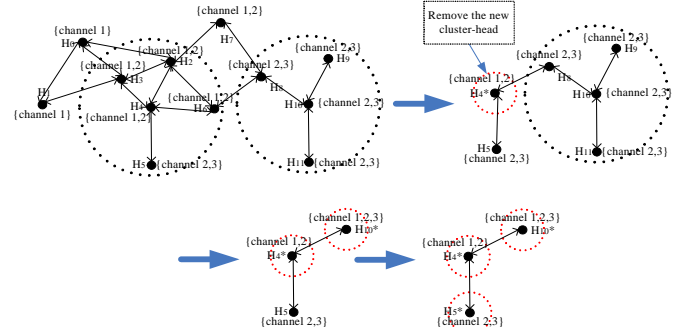Fig. 4: Flow chart of node contraction scheme.

Fig. 5: Control channel selection with node contraction scheme.

The main advantage of this clustering scheme is that it can quickly find the CCC that is suitable for the dynamic spectrum environment, and also reduces the CCC reconstruction overhead. However, it cannot provide the optimal solution as discussed in simulation results in Section 5. To find the optimal solution, we propose a particle swarm optimization method as below.

3.2 Discrete Particle Swarm Optimization (DPSO)

PSO is a population-based optimization method inspired by the birds' flocking behavior [42, 43]. It uses the iterative update of parameters to converge to a global decision through the use of a concept called *particles* [42]. Each particle can be initialized randomly with certain position and velocity, which are then iteratively updated. In this paper, the particles represent different CCC assignment for all CHs.

To use PSO, we rewrite equations (2.1) and (2.2) as,

$$v_{id}^{k+1} = v_{id}^k + c_1 r_1 (p_{id}^k - x_{id}^k) + c_2 r_2 (p_{bd}^k - x_{id}^k) \qquad (3.4)$$

$$x_{id}^{k+1} = x_{id}^k + v_{id}^{k+1} \qquad (3.5)$$

where $i \in \{1, 2, \ldots, S\}$, S represents the population of particle swarm; $d \in \{1, 2, \ldots, D\}$, D is the dimension of search space; and k is the generation step of evolution. Note that each particle i is assigned a fitness value, which can be found by solving the optimization function in equation (3.3). Such a function can be used to retrieve each particle's moving direction and displacement. Equation (3.4) and (3.5) show how each particle updates itself until finally reaching an optimal solution.

In equation (3.4), p_{id}^k represents the personal best position (PBP) where the particle i has the largest fitness value (see equation (3.3)), and p_{bd}^k represents the global best position (GBP) with the largest fitness value among all the p_{id}^k's outputs. By keeping track of the values of PBP and GBP, we can successfully update each particle. We have used two pseudorandom sequences, r_1 and r_2, to reflect the stochastic nature of the algorithm. Both of them follow the uniform distribution over the range [0, 1]. Acceleration coefficients c_1 and c_2 control the distance a particle moves in a single iteration. Typically they are set as 2 in optimization problems.

The current position x_{id}^k obtained from (3.5) is for *continuous* space. However, x_{id}^k cannot be directly obtained from the current velocity in *discrete* space where only 0 or 1 is assigned to x_{id}^k, p_{id}^k, and p_{bd}^k. Therefore, we use a *discrete (binary) version of PSO (DPSO)* [29, 41], to obtain the particle update in equations (3.6) and (3.7) below. In DPSO, we evolve x_{id}^k into the probability of particle update as follows:

$$v_{id}^{k+1} = v_{id}^k + c_1 r_1 (p_{id}^k - x_{id}^k) + c_2 r_2 (p_{bd}^k - x_{id}^k) \qquad (3.6)$$

$$if \ (Sig(v_{id}^k) > r) \ then \ x_{id}^{k+1} = 1$$
$$else \ x_{id}^{k+1} = 0 \qquad (3.7)$$

where $Sig(v_{id}^k) = [1/1 + \exp(-v_{id}^k)]$ denotes the probability of particle evolution and r is a pseudorandom sequence, which obeys a uniform distribution over [0, 1].

In order to use the above DPSO algorithm for control channel selection, we first denote the *spectrum availability matrix of all CHs* as $A_{I \times M}$. We mark all '1' elements in $A_{I \times M}$ in different columns and rows. For example, for $I = 3, M = 3$, the $A_{I \times M}$ matrix is as follows:

$$A_{I \times M} = \begin{bmatrix} \underline{1} & 0 & \underline{1} \\ 0 & \underline{1} & \underline{1} \\ \underline{1} & \underline{1} & \underline{1} \end{bmatrix}$$

This particle contains seven binary '1' numbers, i.e. $D = 7$. Note that *each particle $A_{I \times M}$ presents a solution which assigns several channels to each CH to form control channel.*

Our proposed DPSO algorithm is as follows:

(1) Set $k = 0$, and generate the position x_{id}^0 and velocity v_{id}^0 for each particle, where $x_{id}^0 \in \{0, 1\}$, $v_{id}^0 \in [-V_{max}, V_{max}]$, $1 \le d \le D$.

(2) For each particle, calculate the fitness value based on the optimization function in equation (3.3). Then we get $p_i^0 = [x_{i1}^0, x_{i2}^0, \ldots, x_{iD}^0]$, and $p_b^0 = [x_{b1}^0, x_{b2}^0, \ldots, x_{bD}^0]$, where b denotes the index number of global best fitness particle.

(3) Let $k = k + 1$, and change the status of v_{id}^k according to equation (3.6). If $v_{id}^k > V_{max}$, set $v_{id}^k = V_{max}$; else if $v_{id}^k < -V_{max}$, set $v_{id}^k = -V_{max}$.

(4) Generate a stochastic number r, which obeys uniform distribution over [0, 1], and change the status of x_{id}^k according to equation (3.7).

(5) For each particle i, calculate the fitness value determined by optimization function in equation (3.3). If the new fitness value is larger than p_i^{k-1}, we let $p_i^k = [x_{i1}^k, x_{i2}^k, \ldots, x_{iD}^k]$, else $p_i^k = p_i^{k-1}$. Similarly, if the new fitness value is larger than p_b^{k-1}, we let $p_b^k = [x_{i1}^k, x_{i2}^k, \ldots, x_{iD}^k]$, otherwise, $p_b^k = p_b^{k-1}$.

(6) If the number of iterations reaches the maximum, stop; else, go back to step (3).

4 INTEGRATION OF CHANNEL SELECTION AND SPECTRUM-AWARE ROUTING

Our aim of CRN routing design in *high-mobility, multi-hop, multi-channel* environment is to select appropriate spectrum bands for each CH and member nodes along the path, *with the constraint of maximum link-availability probability and node capacity*. Conventional CRN routing schemes typically assume that: (1) source node first assigns channel in each link before a route is established [8, 44, 45], and (2) nodes have the same spectrum opportunities (SOP), which may not be realistic in CRN.

In this paper, we propose a framework for spectrum aware on-demand routing considering heterogeneous channel conditions in each node. *The proposed routing scheme integrates control channel selection with on-demand route discovery.* The routing in multi-hop CRN includes *intra-cluster* and *inter-cluster* routing processes. The intra-cluster routing occurs in a single cluster, while inter-cluster routing occurs in multiple clusters. The proposed routing scheme contains route discovery /recovery procedures as discussed below.

4.1 Route Discovery

Due to the multi-hop and high-mobility nature, we use spectrum Route REQuest (RREQ) and spectrum Route REPly (RREP) as in [2], to discover paths between nodes via the control channel message exchanges. The *proposed route discovery scheme is integrated with our node-importance-based clustering scheme (Section 2.4), node-contraction or*

DPSO-based control channel selection scheme (Section 3), and data channel assignment scheme (Section 4.3).

Our route discovery process is the same as AODV. However, *to integrate with our node-importance-based clustering scheme,* we design the CRN routing protocol with the Route REQuest (RREQ) packets that contain the fields *<IPS, IPD, metric, intra/inter>.* Here, *<IPS>* and *<IPD>* are the IP addresses of source node and destination node, respectively. The *<metric>* is an important field since it has the product of all link availability probabilities in different links along the routing path (which is actually the path stability metric, see Section 2). *<intra/inter >* indicates whether the destination node is in the same cluster as the source node or not.

When the destination CH receives the first RREQ, it sets up a timer and stores the route information in its routing table. When the timer expires, the destination CH chooses a path *with the largest path availability probability* from all the paths it has collected, and sends the RREP back along that path to the source node. The *Path availability probability* is the product of all the link availability probabilities along the path. Every intermediate CH, while receiving the RREP, sets up a route to destination and assigns a data channel according to a performance metric, *node capacity,* which will be defined in Section 4.3.

4.2 Route Recovery

To handle the link failure issues resulting from the PU activities and node mobility, we adopt the following strategies:

PU awareness: The appearance of a PU may render the region in its vicinity unsuitable for routing. In such cases, the nodes in the affected regions must immediately cease operation in the occupied channel, and explore alternate routes or channel to the destination based on the above routing discovery procedure (section 4.1).

CR user mobility: Source, destination and intermediate nodes mobility may break the route. Even if the route stays connected, nodes may stray into PU activity regions and cause undesirable interference to the licensed users. As a result, the earlier route, formed on the basis of their relative geographical locations, can no longer be considered optimal.

The following three situations cause route failures: (1) link failures among nodes in the source or destination cluster; (2) link failures among intermediate CHs; (3) the source node or the destination node joins a new cluster. The first situation can be handled by our *node-importance-based* CH to recovery the links with the local information of the cluster. The second situation requires the pre-hop CH to broadcast RREQ on the control channel to form a new path, which is achieved in the process of route discovery. The third situation requires the source node to resend RREQ again.

4.3 Channel Assignment Scheme

Similar to the on-demand routing scheme mentioned in [2, 8], we also require that the RREP should be sent on the working control channel of a pre-hop node (or CH). As discussed before, the control channel information of the pre-hop node can be extracted from the RREQ message. If the pre-hop node is a *gateway*, it will broadcast its working control channel information whenever it changes its channel.

The channel assignment strategy has been studied widely. Most conventional schemes focus on QoS requirement, i.e., cumulative delay and channel capacity. In this section, we first discuss the drawback of a *cumulative delay* based routing metric (also known as DORP in [46]), followed by our proposed new routing metric based on *node capacity.*

In [46, 47], the cumulative delay consists of two parts: node delay (DN) and path delay (DP). DN consists of the switching delay ($D_{switching}$) *between* frequency bands, and the backoff delay ($D_{backoff}$) in a frequency band. The DN depends on the number of traversing flows as well as the frequency bands used by them. The switching delay can be represented as [46]:

$$D_{switching} = 2K \cdot \left| Band_M - Band_1 \right| \qquad (4.1)$$

where K is a positive constant (suggested as $10ms/10MHz$ in [8, 46, 47]) and $Band_i$ is the frequency band from node's active band set of M bands. The back off delay is obtained as [47]:

$$D_{backoff}(Num_i) = \frac{1}{(1-p_c)(1-(1-p_c)^{\frac{1}{Num_i-1}})}W_0 \qquad (4.2)$$

where Num_i is number of nodes that are competing for channel access, p_c is probability that a contending node experiences collision, and W_0 is minimum contention window size.

The *cumulative delay* (i.e., *end-to-end routing delay*) only considers the minimum delay of a new flow. The DP does not consider existing active data channel. As a result, the cumulative delay based routing metric proposed in [46, 47] cannot obtain minimum average end-to-end delay for all flows.

We illustrate the proposed channel assignment concept in Fig. 6. In Fig. 6(a), Flow 1's route is established between nodes 4 and 5. Since the destination node assigns channel 1 to Flow 1, node 2 must work on channel 1 in order to forward Flow 1, and it also assigns channel 1 at the receiver side because source node 4 can only work on channel 1. To set up route for a new data flow (denoted as New Flow), node 3 assigns channel 3 at the receiver. Node 2 must assign channel 3 to forward such a new flow. According to equation (4.2), node 2 is supposed to assigns channel 1 in order to reduce backoff delay of DN, compared with the assignment of channel 3. Moreover,

the switching delay of DN with assigning channel 1 and 3 is the same according to equation (4.1). However, assigning channel 1 will increase the entire DP which contains switching delay and backoff delay along the path node 1—> node 2—> node3. Hence, in Fig. 6(a), node 2 will assign channel 3 at the receiver using DORP; whereas, in Fig. 6(b), node 2 will assign channel 1 at the receiver using our proposed routing metric and forward the flow on channel 3.
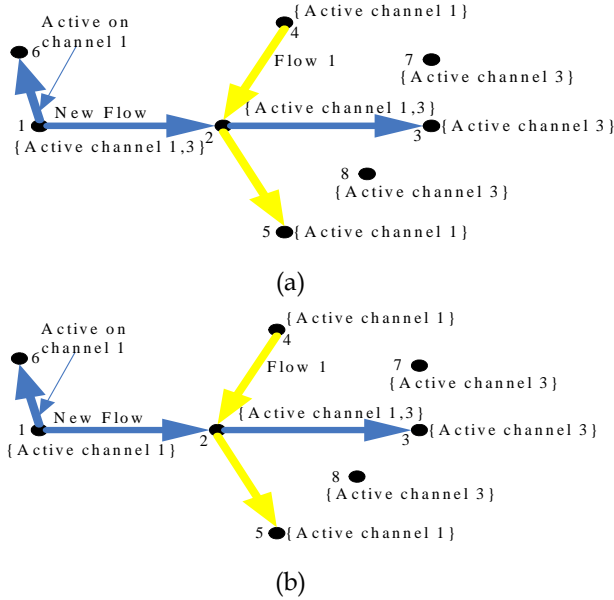

Fig. 6: Channel assignment results: (a) cumulative delay routing metric; and (b) our proposed routing metric.

Since the path is determined by the largest path availability probability, the capacity of each node determines the average end-to-end delay for all flows in CRN. We define node i's *capacity* as

$$\eta_i = \frac{\sum_{j=1}^{M} T_{i,j} b_{i,j}}{\sum_{j=1}^{M} T_{i,j} + D_{switching} + \sum_{j=1}^{M} D_{backoff}(Num_j)} \quad (4.3)$$

where M is the number of active channels for node i, and $T_{i,j}$ is the service time of node i on channel j, which is known to node i. A larger value of η_i can reduce the average end-to-end delay or improve the throughput, as we will see in our experiments in Section 5.

As shown in Fig. 6(b), our proposed *node capacity based* routing strategy assigns channel 1 at the receiver part of node 2 since channel 1 introduces a smaller backoff delay (compared with channel 3) and has a larger node capacity (see equation 4.3). The channel assignment strategy of Fig. 6(b) is better than Fig. 6(a), since node 1 in Fig. 6(a) has a large switching delay and a deaf problem exists between node 1 and node 2. The *join* message and *leave* message should be sent out to avoid this problem. *In summary, the cumulative-delay-based routing metric may increase the* *average end-to-end delay or reduce the throughput, compared to our proposed node capacity metric.*

5. EXPERIMENTAL RESULTS

In this section we discuss the performance of CRN clustering, channel assignment and routing schemes discussed in Sections 2 – 4.

The simulation set up uses 10km×10km×2.5km area, where 10km×10km is the horizontal range, with a vertical range of 2.5km (the height range is [0.5km, 3km]). We consider 10 PUs, 10 available channels, 100 secondary users, and 10 target areas. The transmission range of each CRN node is [0.1km, 3km], and the interference range of a PU is 1km, which are determined by the RF transmit power and receiver sensitivity. The average number of clusters and the connectable probability of the CRN, are calculated by 1000 random deployed scenarios. The average number of clusters tries to show how many clusters are formed with different clustering algorithms; while the connectable probability of the CRN shows the probability that the formed clusters can connect with each other. Since the primary as well as secondary users are deployed randomly, the statistical values are calculated after the nodes fly for a period of 100s.

5.1 CRN Clustering Performance

Figures 7 and 8 compare the performance of the proposed, the Max Node Degree and the Lowest ID clustering schemes. Here, the longevity of the topology structure is $T = 100s$ with link availability probability $P_0 = 0.9$. In Fig. 7, we set the maximum node speed as 50m/s in each direction.

In Fig. 7(a) and Fig. 8(a), we observe that the Lowest ID clustering scheme produces the largest average number of clusters, since it does not consider the topology structure and node importance in CRNs. On the other hand, the Max Node Degree clustering scheme reduces the number of clusters, since it selects the nodes with the largest number of neighbors as CHs. Hence, the Lowest ID clustering scheme that generates more CHs has a larger connectable probability of the whole CRN than the Max Node Degree clustering scheme (see Fig. 7(b) and Fig. 8(b)).

In Figs. 7(a) and 8(a), we also observe that the average number of clusters increases when the number of nodes and maximum speed increases. Since our proposed clustering scheme considers the node degree, it forms the lowest number of clusters which is almost the same as the Max Node Degree scheme. Moreover, our proposed clustering scheme also considers the link availability probability, it generally achieves the highest connectable probability of the CRN which is almost the same as the Lowest ID scheme (see Figs. 7(b) and 8(b)). Note that the Lowest ID scheme forms the largest number of clusters and its performance depends on the location of nodes with lowest ID. Since our proposed clustering scheme

considers not only node degree but also the link availability probability, it could tradeoff between the number of clusters and connectable probability of the CRN.
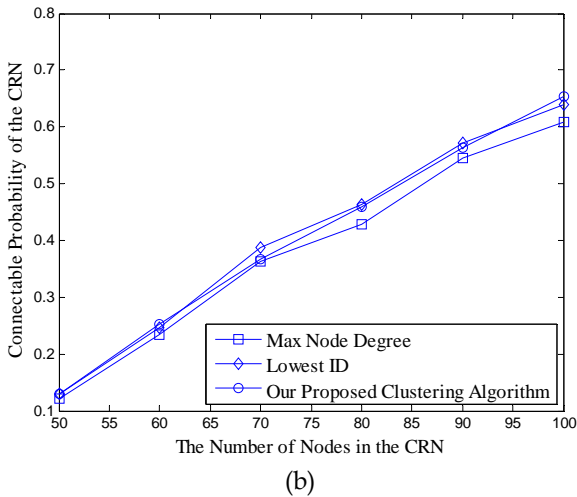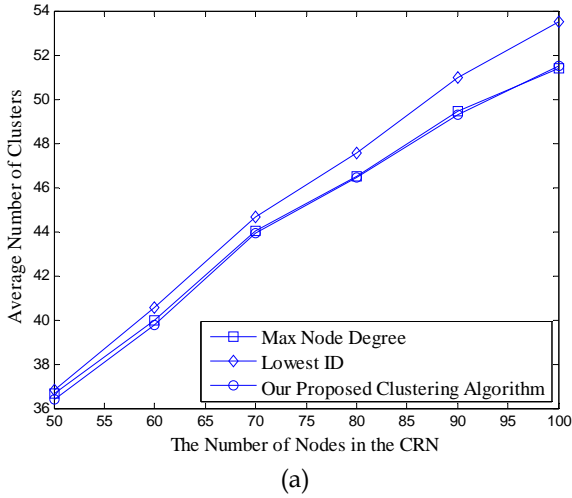

(a)

(b)

Fig. 7: Performance of clustering schemes for varying number of nodes in CRN (a) Average number of clusters, and (b) Connectable probability of the CRN.
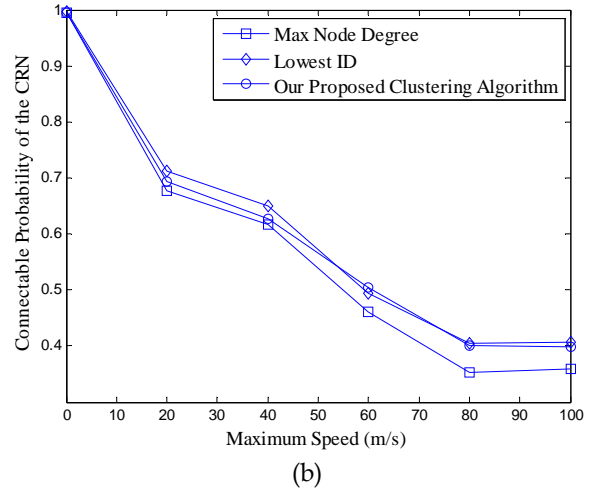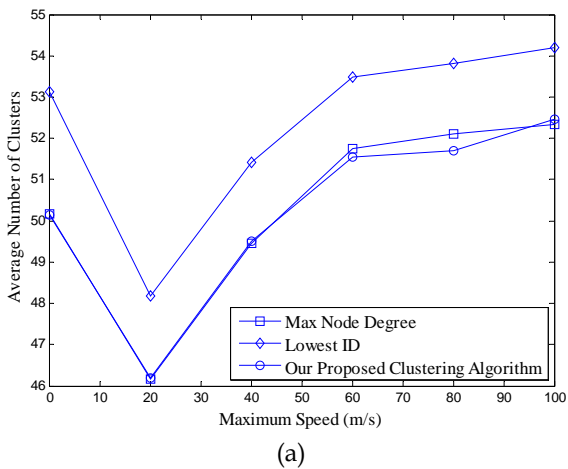

(a)

(b)

Fig. 8: Performance of clustering schemes for maximum node speeds (a) Average number of clusters, and (b) Connectable probability of the CRN.

Therefore, our proposed clustering scheme is more suitable to CRN topology management than the other two schemes as it forms the lowest number of clusters and at the same time achieves the highest connectable probability of the CRN.

5.2 Control Channel Selection Performance

Next, we compare the performance of our node contraction and DPSO control channel selection schemes with the graph coloring scheme [30], which is a typical spectrum allocation scheme in CRNs. For this, we calculate three statistical values: the normalized delay, the normalized throughput, and the optimization function (equation 3.3) for 100 randomly deployed CRN cases. The normalized delay and normalized throughput are:

$$\text{Normalized Delay} = \frac{Delay}{(I-1)t_{hop} + (M-1)t_{sw}}$$

$$\text{Normalized Throughput} = \frac{U_{sum}}{I \times \max\{b_{n,m}, n \in \{0,1,\dots,I-1\}, m \in \{0,1,\dots,M-1\}\}}$$

where Delay was defined in equation (3.1) and U_{sum} was defined in equation (3.2). The performance of three schemes is shown in Figs. 9-12 by varying the number of clusters, available channels, PUs and weight coefficients. The 1-hop transmission time t_{hop} depends on the CCC bandwidth, the packet size, the packet loss rate, etc. During the CCC selection, information about a cluster (ID, position, velocity, and available channels for each node) is stored in a packet. Note that the channels suitable for CCC are non-contiguous and their bandwidth is narrow (10kHz to 100kHz). We therefore set $t_{hop} = 200$ ms and $t_{sw} = 10$ ms [8] in our simulation. In Figs. 9-11 the weighted coefficient χ is 0.5. The particle number is 50 and the number of iteration times is 100 for DPSO scheme in our simulations.
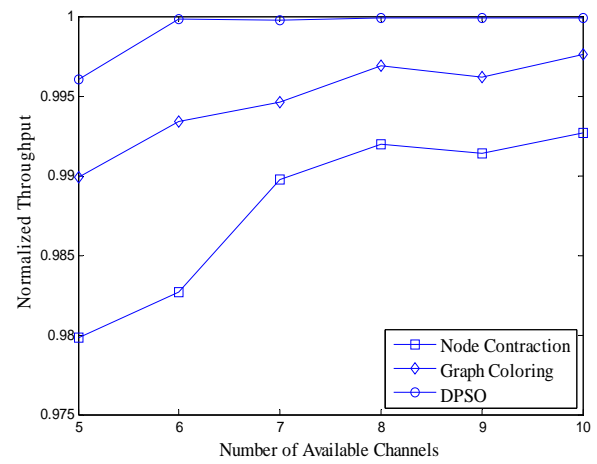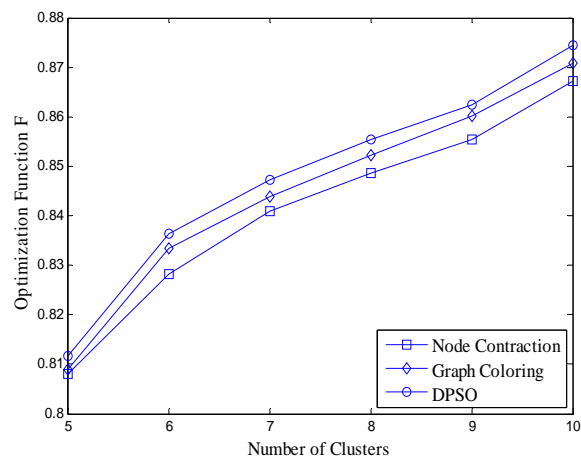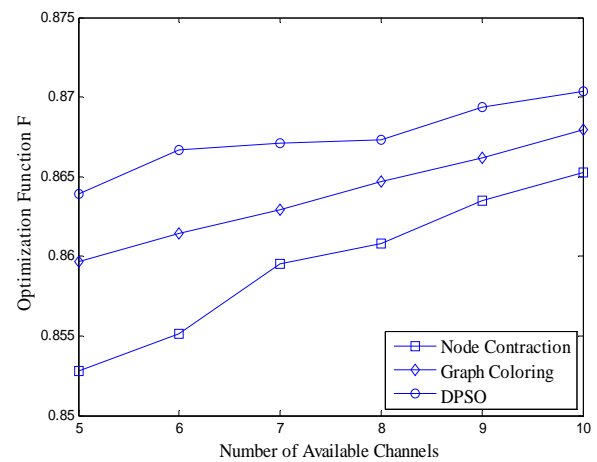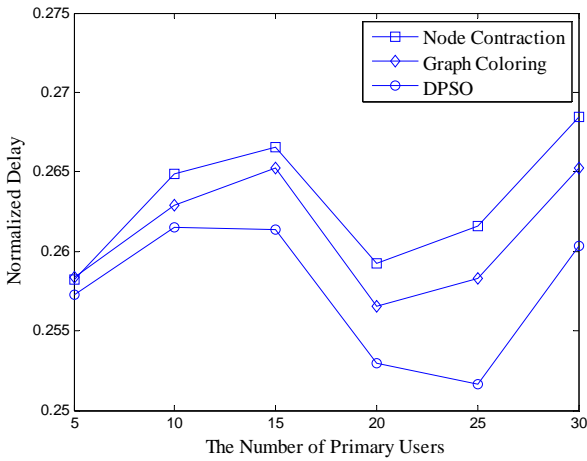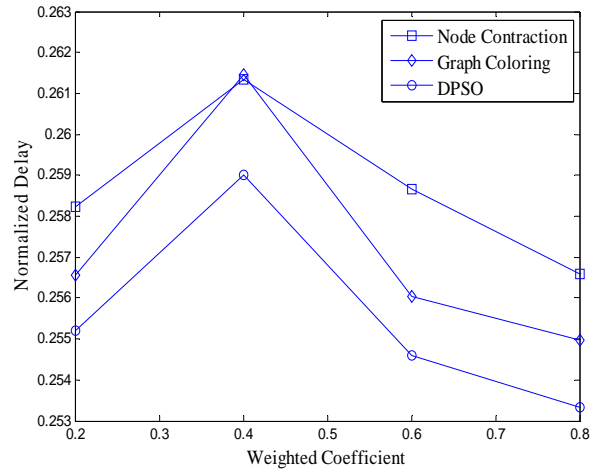
(a)

(b)
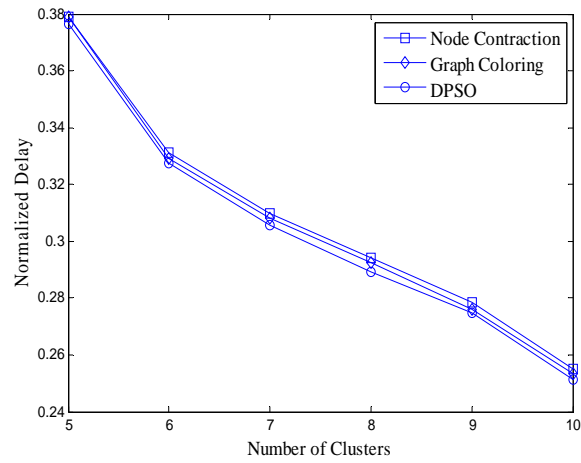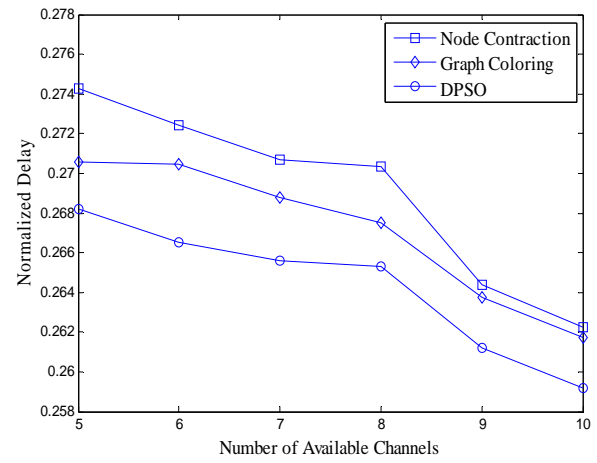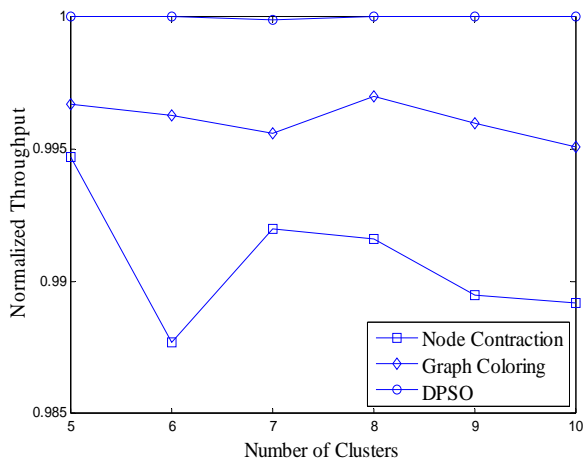
(c)

Fig. 9: Performance of three common control channel selection schemes for varying number of clusters: (a) normalized delay, (b) normalized throughput, and (c) optimization function.
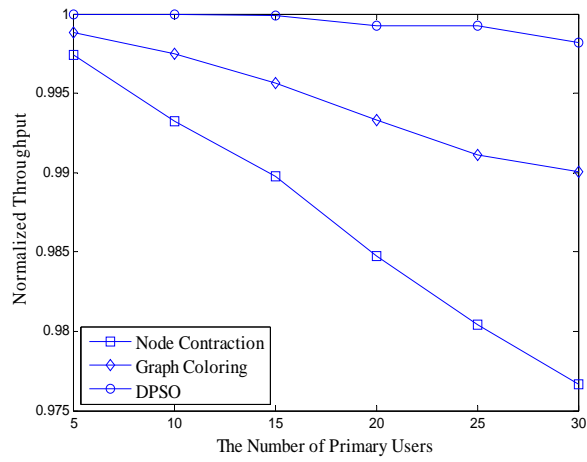
Fig. 10: Performance of three common control channel selection schemes for varying number of available channels: (a) normalized delay, (b) normalized throughput, and (c) optimization function.
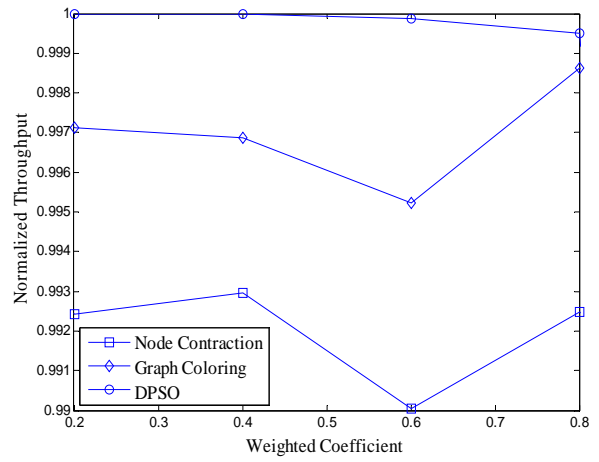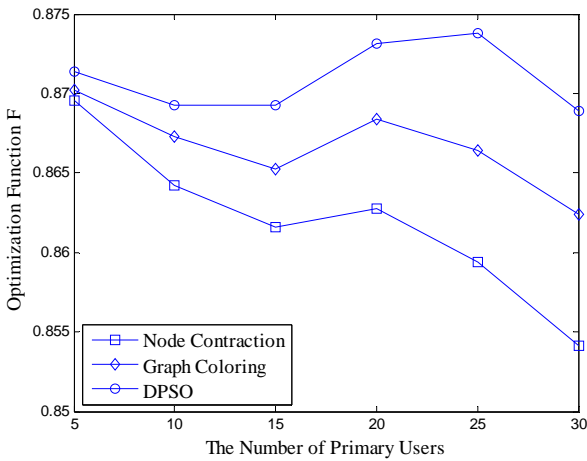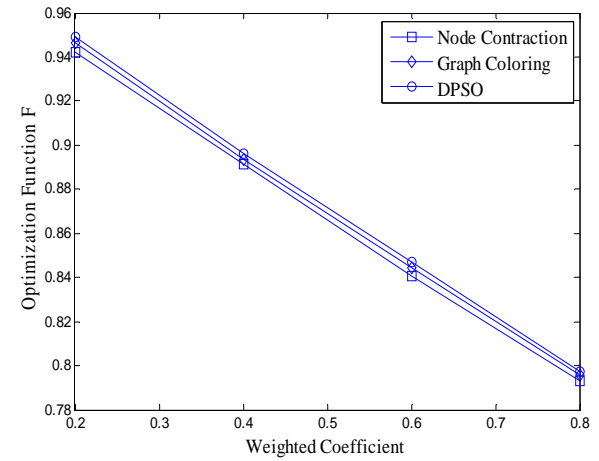
Fig. 11: Performance of three common control channel selection schemes for varying number of PUs: (a) normalized delay, (b) normalized throughput, and (c) optimization function.

Fig. 12: Performance of three common control channel selection schemes for varying values of weighted coefficient χ : (i) normalized delay, (b) normalized throughput, and (c)optimization function.

The DPSO scheme achieves better delay, throughput and optimization function performance than the other two schemes. However, it needs more time to converge to the best solution. Its execution time is a linear function of particle numbers, iteration times, the number of CHs and available channels. The computational complexity of the node contraction and graph coloring schemes is only a linear function of the number of CHs and available channels. The node contraction scheme has the smallest time consumption. In Fig. 4, after labeling out the CH with maximum channel reward, the node contraction scheme assigns a common channel to CHs in its multi-hop neighboring CHs each time. As a result, it consumes less time than the graph coloring scheme, which assigns a common channel to CHs in its 1-hop neighborhood each time (see the flow chart of graph coloring scheme in [30]).

Fig. 13 shows the control channel selection results for the three schemes. A total of 20 CHs are selected with weighted coefficient χ of 0.5. The solid circle represents a single channel working node, while an empty circle represents a gateway. We observe that the node contraction algorithm uses the minimum number of channels to construct control channel, while DPSO uses more channels to optimize the equation (3.3).
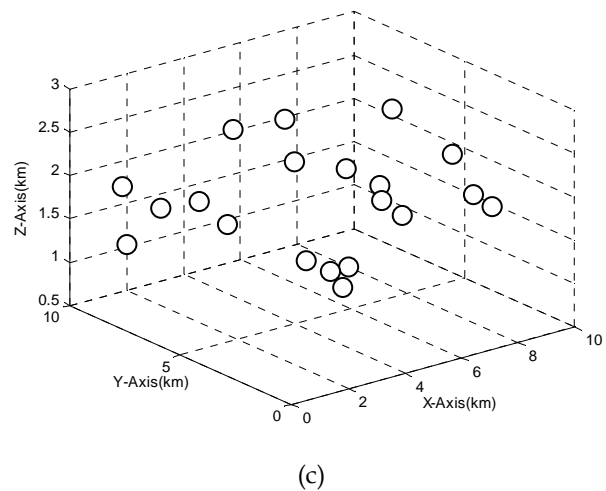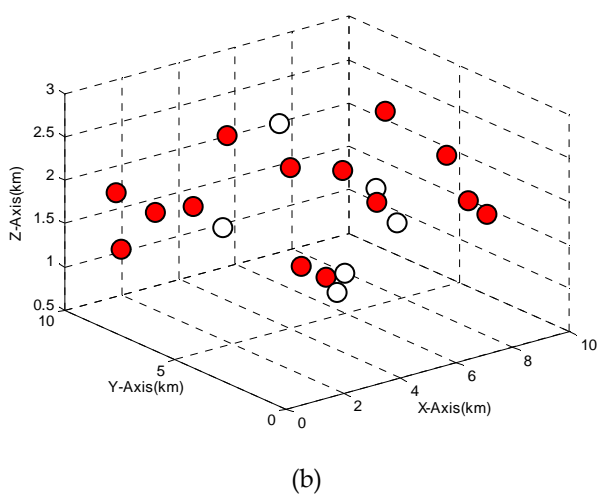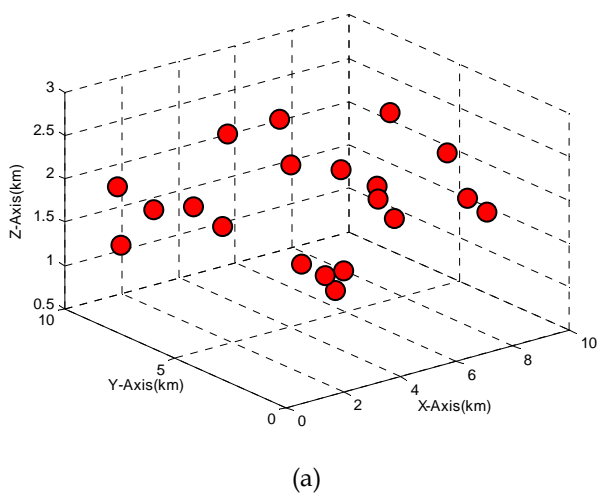
(c)

Fig. 13: Control channel selection results for the three schemes: (a) Node contraction, (b) Graph coloring, and (c) DPSO. The solid circle represents a single channel working node, while an empty circle represents a gateway.

5.3 CRN Routing Performance

In this section, we compare the performance (i.e., average end-to-end delay and packet delivery ratio) of our routing scheme with the *K*-hop distinct [44, 45] and Spectrum aware DORP [46, 47] routing schemes for the static as well as mobile nodes. It is pointed out in [44, 45] that the spectrum assignment should use the *K*-hop distinct scheme in order to reduce the interference and achieve high utilization. On the other hand, [46, 47] argue that the spectrum assignment should consider the cumulative end-to-end delay. However both schemes assume that the CRN nodes are static.

(a) Static Nodes

The simulation parameters are the same as discussed 2nd paragraph of Section 5, and clusters and control channel are formed according to Section 2.4 and Section 3.1, respectively. In total, 100 CRN nodes are randomly deployed, and the source / destination nodes are randomly selected from the nodes. In the simulation, 1-hop transmission time between two nodes A and B is not constant and determined by the hop distance and communication range for the assigned channel. The 1-hop transmission time ($T_{A,m}$) of node A on channel m is given by,

$$T_{A,m} = \frac{b(A,m)}{Dis^2(A,B)} \times T_{hop} \qquad (5.1)$$

The delay variation is due to two reasons: 1) a larger $b(A,m)$ means a higher signal-to-noise ratio (SNR), which can reduce the number of retransmission times; and 2) under the same bit error rate, we can use a higher level digital modulation scheme when $b(A,m)$ is larger. In Fig. 14, the three schemes execute routing protocols under the

(a)

(b)

same topology structure in each scenario, and use the same route paths with different channel assignment schemes for each data flow. Since the source and destination nodes are selected randomly in each scenario, the simulation results show fluctuations.

In Fig. 14, our proposed channel assignment scheme has the lowest end-to-end delay. Since our proposed scheme considers the node capacity (equation 4.3), it can process packets faster, and thus results in lower average end-to-end delay. The DORP scheme takes single flow's cumulative delay as a dominant factor, and tries to reduce the end-to-end delay. It does not consider the node capacity in each flow. On the other hand, the K-hop distinct scheme (we set K=3 in our simulation, which is a typical value [44]) tries to switch between channels to avoid interference. As a result, the cumulative delay increases with number of active flows, which also increases the switching delay in each node, as pointed out in [46].
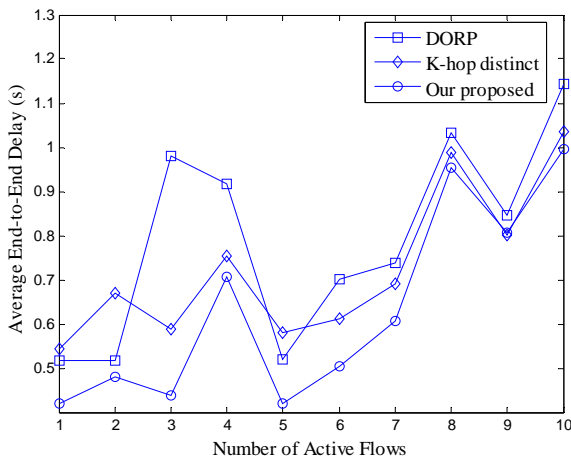

Fig. 14: Performance of three channel assignment schemes for static CRNs.

(b) Mobile Nodes

In our CRN scenario, the airborne nodes move at a high speed. We use our proposed link availability model (see Section 2.3) and select the most stable path with the highest path availability probability. We assume the use of the maximum available transmission range.

Note that the link availability and path availability probability, which were defined in Sections 2.3 and 4.1, respectively, are not used in DORP and K-hop distinct routing schemes [44 - 47]. Those schemes assign channels based on the cumulative end-to-end delay and radio interference, respectively. In our simulations, we use our channel assignment scheme to first find out the channel set with the link availability probability larger than $P_0 = 0.9$ during the next $T = 100$ seconds in RREP process, and then we select the path with the largest node capacity.

Figs. 15 and 16 compare the performance of the proposed routing scheme with the K-hop distinct and

DORP schemes for different maximum node speeds and number of active flows. In Fig. 15, only one flow is transmitted. We observe that our proposed routing scheme has the lowest average end-to-end delay (see Fig. 15(a)) and highest packet delivery ratio (see fig. 15(b)) when the node speed varies from 10m/s to 100m/s. This is because our channel selection scheme considers the *node capacity* and tries to select a channel with maximal data processing capacity for packet transmission. Since the initial conditions (such as the initial position and velocity of source and destination nodes, and the target position) are randomly selected, the simulation results fluctuate in different dimensions (X-axis). The K-hop distinct scheme sometimes performs better than the DORP scheme, depending on the number of hops on the route. Since a route with a larger number of hops often has more interference; the K-hop distinct scheme performs better as it reduces the interference.

Fig. 16 illustrates that the proposed routing scheme generally has the best average end-to-end delay and packet delivery ratio for varying number of active flows. We have used the maximum node speed of 20 m/s in each direction. Since our proposed routing scheme considers the node capacity, its packet delivery ratio is three times compared with DORP and K-hop distinct schemes when the number of active flows is 6 in Fig. 16(b)). As a result, the queuing delay caused by its own packets increases the average end-to-end delay in Fig. 16(a) for this case. We observe a similar behavior in Fig. 16(a) for the K-hop distinct routing scheme when the number of active flows in 8. From Fig. 16(b), we observe that our proposed routing scheme has the highest packet delivery ratio, except when the number of active flows is 8 and 9. For these two values of active flows, the K-hop distinct scheme performs the best. A larger number of hops in the route in our scheme may introduce more interference which causes more packets losses. However, our proposed scheme delivers the packet at a faster rate.
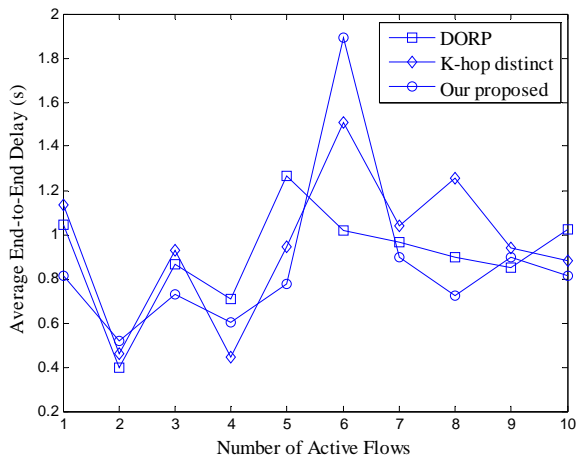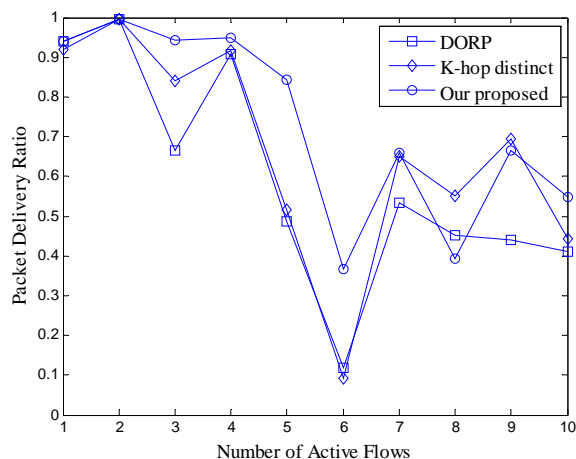

(a)
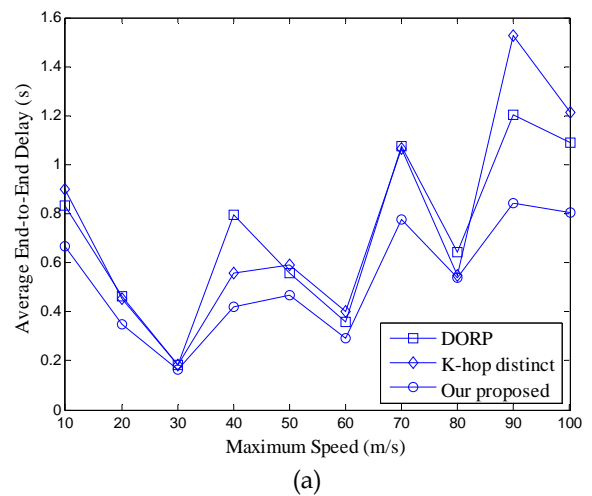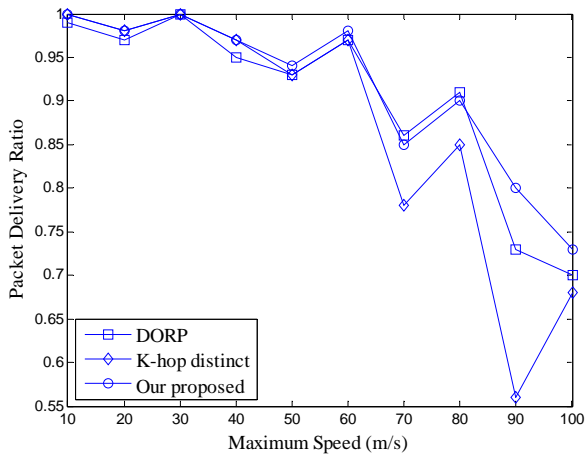
Fig. 15: Performance of three channel assignment schemes for mobile CRNs for maximum node speed in each direction: (a) average end-to-end delay, and (b) packet delivery ratio.

Fig. 16: Performance comparison of three channel assignment schemes for mobile CRNs for a number of active flows: (a) average end-to-end delay, and (b) packet delivery ratio.

6. CONCLUSIONS

In this paper, we discussed a novel routing scheme for a high-mobility CRN scenario consisting of UAVs for surveillance, by considering the path stability and node capacity. We establish the CRN path based on link availability probability. Such a routing is integrated with a clustering scheme which considers the node importance degree. We also proposed two novel control channel selection schemes based on the node contraction and DPSO algorithm. Our simulation results showed that the DPSO has the best performance, while the node contraction scheme has the smallest computational complexity. When we extend our 2-hop cluster coverage to multi-hop coverage cluster, there will be more information exchanged among multi-hop neighboring nodes and produce more overhead in the cluster formation process. However, the number of clusters will dramatically decrease, which will reduce the computation complexity of control channel selection process and the hop length of the route.

Our proposed routing scheme integrates the on-demand routing with dynamic channel assignment. Since the path is determined by the largest path availability probability, the node's processing capacity determines the average end-to-end delay and packet delivery ratio for all data flows. Our results show that our proposed routing CRN protocol has the lowest average end-to-end delay or the largest packet delivery ratio for high mobile cases, compared with two other popular CRN routing schemes, i.e., K-hop distinct routing and DORP.

Since the high mobility of airborne nodes has adverse impact on data transmission due to high link-disrupting rate, we designed the cluster formation and common control channel selection schemes to find out the stable routes to realize multi-hop communications.

The proposed schemes will provide a reliable communication for search or surveillance applications. These schemes will also support stable and low-delay speech, image, and video data transmission. Our future work will investigate the control channel selection scheme in a 3-D physical terrain based on space segmentation algorithms, as well as the multimedia transmission performance in such a CRN routing scheme.

ACKNOWLEDGEMENT

REFERENCES

[1] Federal Communications Commission (FCC), "Spectrum policy task

force report," Report, Et docket no. 02-135, Nov. 2002.

[2] H. Ma, L. Zheng, X. Ma, and Y. Luo, "Spectrum Aware Routing for Multi-hop Cognitive Radio Networks with a Single Transceiver," in the Proc. of IEEE conference, CrownCom2008, pp. 1-6.

[3] A. M. James, "A Link-quality-aware Graph Model for Cognitive Radio Network Routing Topology Management," Thesis, Rochester Institute of Technology, pp. 1-4, 2007.

[4] H. Khalife, S. Ahuja, N. Malouch, and M. Krunz, "Probabilistic Path Selection in Opportunistic Cognitive Radio Networks," in the proc. of IEEE conference, Globecom2008, pp. 1-5.

[5] M. Pan, R. Huang, and Y. Fang, "Cost Design for Opportunistic Multi-Hop Routing in Cognitive Radio Networks," in the proc. of IEEE conference, MILCOM2008, pp. 1-7.

[6] I. F. Akyildiz, W. Lee, M. C. Vuran, and S. Mohanty, "Next Generation/Dynamic Spectrum Access/Cognitive Radio Wireless Networks: a Survey," Computer Networks, vol. 50, no. 13, pp. 2127-2159, 2006.

[7] G. Zhu, I. F. Akyildiz, and G. Kuo, "STOD: A Spectrum-Tree Based On-Demand Routing Protocol for Multi-hop Cognitive Radio Networks," in the proc. of IEEE conference, Globecom2008, pp. 1-5.

[8] G. Cheng, W. Liu, Y. Liu, and W. Cheng, "Spectrum Aware On-demand Routing in Cognitive Radio Networks," in the proc. of IEEE conference, DySPAN2007, pp. 571-574.

[9] M. Gerharz, C. de Waal, M. Frank, and P. Martini, "Link Stability in Mobile Wireless Ad Hoc Networks," in the proc. of IEEE conference, LCN2002. pp. 30-39.

[10] T. Camp, J. Boleng, and V. Davies, "A Survey of Mobility Models for Ad Hoc Network Research," Wireless Communication & Mobile Computing, vol. 2, no. 5, pp. 483-502, 2002.

[11] M. K. Jeya Kumar and R. S. Rajesh, "A Survey of MANET Routing Protocols in Mobility Models," International Journal of Soft Computing, vol. 4, no. 3, pp. 136-141, 2009.

[12] H. Cheng, J. Cao, X. Wang, S. K. Das, and S. Yang, "Stability-Aware Multi-Metric Clustering in Mobile Ad hoc Networks with Group Mobility," Wireless Communications and Mobile Computing, no. 9, pp.759-771, 2009.

[13] A. A.-Kai and R.-H. Jan, "The r-Neighborhood Graph: An Adjustable Structure for Topology Control in Wireless Ad Hoc Networks," IEEE Trans. Parallel and Distributed Systems, vol. 18, no. 4, pp. 536-549, 2007.

[14] A. Ephremides, J. E. Wieselthier, and D. J. Baker, "A Design Concept for Reliable Mobile Radio Networks with Frequency Hopping Signaling," in the proc. of IEEE conference, vol. 75, no.1, pp. 56-73, 1987.

[15] T. Chen, H. Zhang, Marcos D. Katz, and Z. Zhou, "Swarm Intelligence Based Dynamic Control Channel Assignment in CogMesh," in the proc. of IEEE Workshop, ICC, pp. 123-128, 2008.

[16] J. Zhao, H. Zheng, and G.-H. Yang, "Distributed Coordination in Dynamic Spectrum Allocation Networks" in the proc. of IEEE conference, pp. 259-268, 2005.

[17] T. Chen, H. Zhang, G. Maggio, and I. Chlamtac, "Topology Management in CogMesh: A Cluster-Based Cognitive Radio Mesh Network," in the proc. of IEEE CogNet Workshop in Conjunction with IEEE ICC, Glasgow Scotland, 2007.

[18] K. Bian and J. Park, "Segment-Based Channel Assignment in Cognitive Radio Ad Hoc Networks," in the proc. of CROWNCOM, Orlando USA, Aug. 2007.

[19] A. K. Yau, P. Komisarczuk, and P. D. Teal, "C2net: A Cross-Layer Quality of Service (QOS) Architecture for Cognitive Wireless Ad Hoc Networks," in the proc. of IEEE conference, ATNAC2008, pp. 306-311.

[20] E. Gelenbe, P. Liu, and J. Lainé, "Genetic Algorithms for Route Discovery," IEEE Trans. Systems, Man, and Cybernetics-Part B: Cybernetics, vol. 36, no. 6, pp. 1247-1254, Dec. 2006.

[21] Ricardo Lent, "Linear QoS Goals of Additive and Concave Metrics in Ad Hoc Cognitive Packet Routing," IEEE Trans. Systems, Man, and Cybernetics-Part B: Cybernetics, vol. 36, no. 6, pp. 1255-1260, Dec. 2006.

[22] Q. He and H. Zhou, "Research on the Routing Algorithm Based on QoS Requirement for Cognitive Radio Networks," in the proc. of IEEE conference, CSSE2008, pp. 1114-1117.

[23] Y. Thomas Hou, Y. Shi, and H. D. Sherali, "Spectrum Sharing for Multi-Hop Networking with Cognitive Radios," IEEE Journal on Selected Areas in Communications, vol. 26, no.1, pp. 146-155, Jan. 2008.

[24] Y. Shi, Y. T. Hou, and S. Kompella, "A Cross-Layer Approach to Multi-Hop Networking with Cognitive Radio," in the proc. of IEEE conference, MILCOM2008, pp. 1-7.

[25] H. Hassanein, H. Du, and C. Yeh, "Robust Route Establishment in High-Mobility MANETs," in the International Computer Engineering Conference, ICENCO2004, pp. 74-80.

[26] M. Zarei, K. Faez, J. Moosavi Nya, and M. Abbaszadeh Meinagh, "Route Stability Estimation in Mobile Ad Hoc Networks using Learning Automata," in the proc. of 16th Telecommunications Forum TELFOR2008, pp. 76-79.

[27] W. Zhu, M. Song, and S. Olariu, "Integrating Stability Estimation into Quality of Service Routing in Mobile Ad-hoc Networks," in the proc. of IEEE conference, IWQoS2006, pp. 122-129.

[28] W. ALMobaideen. "SPDA: Stability Based Partially Disjoint AOMDV," European Journal of Scientific Research, vol. 27, no. 3, pp. 342-348, 2009.

[29] Z. Zhao, S. Xu, S. Zheng, and Y. Niu. "Cognitive Radio Decision Engine Based on Binary Particle Swarm Optimization," Acta Physica Sinica, vol. 58, no. 7, pp. 5118-5125, 2009.

[30] C. Peng, H. Zheng, and B. Y. Zhao, "Utilization and Fair in Spectrum Assignment for Opportunistic Spectrum Access," Mobile Networks Application, vol. 2006, no. 11, pp.555-576, 2006.

[31] H. Chang and K. Chen, "Auction-Based Spectrum Management of Cognitive Radio Networks," IEEE Transactions on Vehicular Technology, vol. 59, no. 4, pp. 1923-1935, 2010.

[32] M. Ma and D. H. K. Tsang. "Joint Spectrum Sharing and Fair Routing in Cognitive Radio Networks," in the Proc. of IEEE conference, CCNC2008, pp. 978-982.

[33] A. Bruce McDonald and T. F. Znati, "A Mobility-Based Framework for Adaptive Clustering in Wireless Ad Hoc Networks," IEEE Journal on Selected Areas in Communications, vol. 17, no. 8, pp. 1466-1487, 1999.

[34] A. Bruce McDonald and T. F. Znati, "A Path Availability Model for Wireless Ad-Hoc Networks," in the proc. of IEEE conference, WCNC1999, vol. 1, pp.35-40.

[35] S. Jiang, D. He, and J. Rao, "A Prediction-based Link Availability Estimation for Mobile Ad Hoc Networks," in the proc. of IEEE conference, INFOCOM2001, pp.1745-1752.

[36] X. Wu and E. Bertino, "An Analysis Study on Zone-Based Anonymous Communication in Mobile Ad Hoc Networks," IEEE Transactions on Dependable and Secure Computing, vol. 4, no. 4, pp.252-265, Oct. 2007.

[37] http://en.wikipedia.org/wiki/Lyapunov%27s_central_limit_theorem.

[38] Q. Guan, F. R. Yu, S. Jiang, and G. Wei, "Prediction-Based Topology Control and Routing in Cognitive Radio Mobile Ad Hoc Networks," IEEE Transactions on Vehicular Technology, vol. 59, no. 9, pp. 4443-4452, 2010.

[39] K. R. Chowdhury and M. D. Felice, "Search: A routing protocol for mobile cognitive radio ad-hoc networks," Computer Communications, vol. 32, no. 18, pp. 1983-1997, 2009.

[40] H. Shiang and M. v. d. Schaar, "Queuing-Based Dynamic Channel Selection for Heterogeneous Multimedia Applications Over Cognitive Radio Networks," IEEE Transactions on Multimedia, vol. 10, no. 5, pp. 896-909, 2008.

[41] Y. Liu and X. Gu, "Skeleton-Network Reconfiguration Based on Topological Characteristics of Scale-Free Networks and Discrete Particle Swarm Optimization," IEEE Trans. Power Systems, vol. 22, no. 3, pp. 1267-1274, 2007.

[42] J. Kennedy and R.C. Eberhart, "Particle Swarm Optimization," in the proc. of IEEE Neural Networks Conference, vol. 1995, no. 4, pp. 1942-1948, 1995.

[43] Y. Liu, X. Gu, "Reconfiguration of network skeleton based on discrete particle-swarm optimization for black-start restoration ," in IEEE Power Engineering Society General Meeting, October 2006. Montreal, Que.

[44] M. X. Gong and S. F. Midkiff, "Distributed Channel Assignment Protocols: A Cross-Layer Approach," in the proc. of IEEE conference, WCNC2005, pp. 2195-2200.

[45] M. X. Gong, S. F. Midkiff, and S. Mao, "Design Principles for Distributed Channel Assignment in Wireless Ad Hoc Networks," in the proc. of IEEE conference, ICC2005, vol. 5, pp. 3401-3406.

[46] G. Cheng, W. Liu, Y. Li, and W. Cheng, "Joint On-demand Routing and Spectrum Assignment in Cognitive Radio Networks," in the proc. of IEEE conference, ICC2007, pp. 6499-6503.

[47] Z. Yang, G. Cheng, W. Liu, W. Yuan and W. Cheng, "Local Coordination Based Routing and Spectrum Assignment in Multi-hop Cognitive Radio Networks," Mobile Net. Appl., no.13, pp. 67-81, 2008.